Journal of King Saud University – Science 35 (2023) 102454

HOSTED BY

Contents lists available at ScienceDirect

Journal of King Saud University – Science

journal homepage: www.sciencedirect.com

Original article

Isolation of oleanolic acid from *Lavandula stoechas* and its potent anticancer properties against MCF-7 cancer cells via induced apoptosis

Hafiz Majid Rasheed [a], Umar Farooq [a], Kashif Bashir [a], Fazli Wahid [b], Taous Khan [a,*], Ameer Khusro [c,*], Mário Gajdács [d], Saad Alghamdi [e], Ahad Amer Alsaiari [f], Mazen Almehmadi [f], Sher Afzal [g], Muhammad Umar Khayam Sahibzada [h,*]

[a] Department of Pharmacy, COMSATS University Islamabad, Abbottabad Campus, 22060, Pakistan
[b] Department of Biomedical Sciences, Pak-Austria Fachhochschule: IAST, Mang, Khanpur Road, Haripur 22620, Pakistan
[c] Centre for Research and Development, Department of Biotechnology, Hindustan College of Arts & Science, Padur, OMR, Chennai 603103, India
[d] Department of Oral Biology and Experimental Dental Research, Faculty of Dentistry, University of Szeged, 6720 Szeged, Tisza Lajos krt. 63., Hungary
[e] Laboratory Medicine Department, Faculty of Applied Medical Sciences, Umm Al-Qura University, P.O. Box.715, Makkah 21955, Saudi Arabia
[f] Department of Clinical Laboratory Sciences, College of Applied Medical Sciences, Taif University, P.O. Box 11099, Taif 21944, Saudi Arabia
[g] Soil and Water Testing Laboratory, Attock, Pakistan
[h] Department of Pharmacy, The Sahara University, Narowal, Punjab, Pakistan

ARTICLE INFO

Article history:
Received 25 May 2022
Revised 1 September 2022
Accepted 14 November 2022
Available online 21 November 2022

Keywords:
Anticancer
Apoptosis
Caspases
Fluorescent microscopy
Lavandula stoechas
Oleanolic acid

ABSTRACT

Medicinal plants are natural resources of diversified therapeutic metabolites. *Lavandula stoechas* has been used traditionally for the management of different metabolic disorders. However, studies on the anticancer characteristics of certain bioactive compounds present in this plant are very limited. In view of this, the aim of the present study was to isolate oleanolic acid (a triterpenoid) from *L. stoechas* and assess its anticancer trait against breast carcinoma cells (MCF-7) via induced apoptosis. Initially, oleanolic acid was isolated from the ethyl acetate fraction of *L. stoechas* using standard extraction protocols. Furthermore, the structure of compound was established using mass spectrometry, FT-IR, ^{1}H NMR, and 2D NMR (HSQC) techniques. *In vitro* antiproliferative effect of oleanolic acid was assessed against breast carcinoma cells (MCF-7 and MDA-MB-231) and non-cancerous cells (BHK-21) using the MTT assay. Oleanolic acid showed prominent cytotoxicity of 72.44 ± 3.33 and 78.55 ± 2.67 % against MCF-7 and MDA-MB-231 cells with IC_{50} values of 13.09 and 160.22 µg/mL, respectively. Moreover, the compound showed negligible toxicity against the BHK-21 cell line. Furthermore, the apoptotic features in oleanolic acid-treated MCF-7 cells were determined using fluorescent microscopy, which showed typical nuclear condensation, increased ROS generation, and the loss of outer mitochondrial membrane potentials. The levels of activated caspases in MCF-7 cancer cells were estimated using a fluorescent kit, showing a significant increment in caspase-9 and caspase-7 for oleanolic acid-treated MCF-7 cells. Moreover, oleanolic acid showed down-regulation of the *Bcl2* and *PDGF* genes. Our findings demonstrated the pivotal role of oleanolic acid as pronounced anticancer agent against MCF-7 cell lines by inducing apoptotic mechanism via intrinsic pathway.

1. Introduction

Breast carcinoma is the foremost cause of cancer-associated mortalities in females. More than 2 million women are diagnosed with breast cancer annually worldwide (He et al., 2020). On the other hand, males are less prone to this disease and constitute about 1 % of the total diagnosed cases overall (Siegel et al., 2015). Breast cancer-related mortalities continue to increase, especially in developing countries, including Pakistan (Bines and Eniu, 2008). Breast cancer is commonly caused due to the

* Corresponding authors.
E-mail addresses: taouskhan@cuiatd.edu.pk (T. Khan), armankhan0301@gmail.com (A. Khusro), umar.sahibzada@gmail.com (M. Umar Khayam Sahibzada).
Peer review under responsibility of King Saud University.

Production and hosting by Elsevier

https://doi.org/10.1016/j.jksus.2022.102454
1018-3647/

down-regulation of DNA repair genes, proto-oncogenes, tumour suppressor genes, inflammatory cytokines, growth factor receptors, nuclear factor kappa-B, interleukins, and tumor necrosis factors. Furthermore, the up-regulation of growth factor receptors (epidermal-, platelet derived-, and vascular-endothelial growth factor) as well as HER2/neu, and down regulation of p53, ataxia telangiectasia mutated, and breast cancer gene 1/2 genes may also lead to breast cancer (Sporikova et al., 2018).

Recently, compounds isolated from medicinal plants have been reported as promising anticancer agents at cellular, pre-clinical, and clinical levels (Petrovska, 2012; Latha et al., 2019; Batool et al., 2022). Some of these plant-based medicines like vinca alkaloids, podophyllotoxin, and paclitaxel are already in clinical use for the management of various types of cancers, including breast cancer. However, these medicines present with some considerable limitations like non-selectivity, rapid clearance, low bioavailability and efficacy, restriction in metastasis, and expensive doses (Gala et al., 2020).

Oleanolic acid is one of the most common biologically active pentacyclic triterpenoids, which is found in more than 1600 plant species (Li et al., 2015). It possesses diverse therapeutic activities such as anti-diabetic, antioxidant, antiviral, hepato-protective, anti-inflammatory, antimicrobial, and anti-proliferative effects (Shanmugam et al., 2014). The anticancer effects of oleanolic acid have been documented against several cancer cell lines viz. lung, breast, liver, pancreatic, colon, gallbladder cancers, and hematological malignancies (Zhang et al., 2007). The anticancer properties of oleanolic acid are attributed to the inhibition of cells growth, initiation of apoptosis, suppression of invasion, and migration (Ziberna et al., 2017).

Lavandula stoechas L. belongs to the Lamiaceae family and is locally known as 'Ustukhuddoos'. *L. stoechas* is distributed throughout the World especially in Asia, Africa, and Europe (Siddiqui et al., 2016). Traditionally, it is used for the treatment of chills, inflammation, digestive track disorders, headache, depression, and diabetes. L. stoechas has been reported to contain ursolic acid, oleanolic acid, vergatic acid, sitosterol, amyrin, lupeol, erythrodiol, flavonoids, and derivatives of longipinane. *L. stoechas* has shown anti-convulsant, anti-spasmodic, anti-oxidant, anti-inflammatory, anti-diabetic, and cytotoxic potentials (Siddiqui et al., 2016). Oleanolic acid and its synthetic derivatives have shown anticancer properties against MCF-7 cells in the past (Khwaza et al., 2020). However, the anti-cancer activities of oleanolic acid against non-cancerous cells have not been explored. In the current study, an attempt was undertaken to isolate oleanolic acid from *Lavandula stoechas* (major constituent on the basis of LC-MS/MS analysis of extract) through different analytical techniques and to evaluate its anticancer activities against breast cancer cell lines and non-cancer BHK-21 cells via an MTT assay, and to ascertain the molecular mechanism of action through caspase activation and polymerase chain reaction.

2. Materials and methods

2.1. Plant materials, extraction, and fractionation

Flowers of *L. stoechas* were purchased from the local market of Lahore, Pakistan. Plant material was confirmed by a plant taxonomist and the voucher specimen (CUHA-196) was submitted in "Environmental Sciences Department, COMSATS University, Islamabad (Abbottabad Campus)". The plant material (10 Kg) was pulverized and macerated in methanol (40 L) for 21 days. The maceration process was repeated for further 7 days using fresh solvent (40 L). The obtained methanolic mixture was filtered through muslin cloth, followed by Whatman filter paper (Said et al., 2020). The filtrates were pooled and dried at 40 °C under reduced pressure using rotary evaporator (Rotavapor R-300 system, Switzerland) (Nana et al., 2019). The extract (800 g) was mixed with distilled water (800 mL) and apportioned sequentially (5 times) with hexane, chloroform, ethyl acetate, and butanol (Rasheed et al., 2021). All pooled solvents from each partitioned extract were dried separately by rotary evaporator at 40 °C to obtain the respective fractions.

2.2. Isolation of compound

LC-MS/MS analysis of both bioactive crude extract and ethyl acetate fraction gave prominent peak with m/z 455.05 at a retention time of 8.06 min, indicating the molecular formula and fragmentation pattern of tripterpenoids. Based on the pharmacological activity and spectrometric results, the ethyl acetate fraction from crude extract of *L. stoechas* was further selected for the isolation of possible anti-breast cancer compounds. The ethyl acetate fraction (3 g) was subjected to column chromatography on silica gel and eluted with different ratios of *n*-hexane and ethyl acetate (10:0, 9:1, 8.5:1.5, 8:2, 7:3, 5:5, 3:7, 2:8, 1:9, and 0:10 v/v). Elution was monitored by TLC and the eluent flasks were pooled together based on similar pattern of TLC spots into a total of 60 fractions. From these sub-fractions, fraction 1–14 (600 mg) contained isolated compound and were chromatographed (purification) on a flash silica gel (Scharlau, Spain; 230–400 mesh) using *n*-hexane and ethyl acetate (10:0, 9.5:0.5, 9:1, 8:2, 7:3, 6:4, and 5:5 v/v) as eluent. The sub-sub-fractions 5–9 yielded the compound (22 mg), which was investigated further for anti-breast cancer activities.

2.3. Characterization of isolated compound

2.3.1. Mass spectrometry

For HR-MS determination, LC-MS/MS analysis was carried out using a U-HPLC Luna Omega reverse-phase column (C18; 50 mm × 2.1 mm, and 1.6 µm) (Phenomenex, USA) connected with a Thermo Velos Pro-ESI trap orbitrap mass-spectrometer (hybrid ion) in positive ion mode (Thermo Fisher Scientific, Germany). A gradient program was set using formic acid (0.1 %) in water (the solvent A), and in acetonitrile (the solvent B). The spectra were recorded in a m/z range of 110–2000, dissociation energy (collision-induced) of 35 V and resolution of 30,000 half maximum, and full width. The software (thermo XCalibur) was employed for data attainment, analyses, and interpretation of the results.

2.3.2. Fourier transform-infrared (FT-IR) spectroscopy

FT-IR analysis was carried out for confirming the presence of functional groups in the isolated compounds. The FTIR measurements of the compounds were recorded on an FT-IR spectrophotometer (Model: IRPrestige-21, SHIMADZU, Japan). All the spectra were acquired through attenuated total reflection method at room temperature using OPUS 5.5 software. A solid sample of the compound was cast on a diamond ATR-FTIR crystal plate and was scanned in between 400 and 4000 cm^{-1} at the resolution of 4 cm^{-1} for investigation. The consequent peaks were then compared with previously published data of functional groups.

2.3.3. Nuclear magnetic resonance (NMR) spectroscopy

NMR analyses (^{1}H NMR and 2D NMR) were performed on a Bruker Avance III HD spectrophotometer (500 MHz) at 22 °C in deuterated DMSO (DMSO d_6) using tetramethylsilane as an internal standard. Chemical shifts were measured in ppm and the coupling constant (J) were expressed in Hertz (Hz) values.

2.4. anti-proliferative activity of oleanolic acid

Two breast carcinoma (MCF-7 and MDA-MB-231) and one non-cancerous (BHK-21) cell line were obtained from American Type Cell Culture (ATCC, MD, USA). These cells were sustained (at 37 °C) in a humid atmosphere of 95 % O_2 and 5 % CO_2 in DMEM media having fetal bovine serum (10 %) and 100 IU/mL of penicillin as well as 100 μg/mL of streptomycin. The anti-proliferative activity of the oleanolic acid was tested on MCF-7, MDA MB 231, and BHK-21 cells using dimethylthiazol diphenyltetrazolium bromide (MTT) assay (Rasheed et al., 2021). Cells at the concentration of 10,000 cells per well were plated into a 96-well plate and permitted to attach overnight. Cells were then incubated with different concentrations of oleanolic acid (31.25–500 μg/mL) and doxorubicin (5–100 μg/mL) for 48 h. DMSO (0.062–1 %) was used as control for all the test samples. After the incubation, the medium was aspirated and 100 μL of the fresh medium containing MTT dye (5 mg/mL) was added to these cells and incubated for further 4 h, followed by the addition of 100 μL of DMSO as solubilizing agent. Absorbance of the dissolved formazan crystals was recorded at 492 nm using microplate reader (Chem plate reader CR-201, China) and viability of cells were estimated. The IC_{50} values were determined using a software (CompuSyn, Version 1.0; ComboSyn, USA). Furthermore, the selectivity index (SI) values of oleanolic acid and doxorubicin were calculated using following formula:

$$SI = IC_{50}\text{value of normal cells}/IC_{50}\text{value of cancer cells}.$$

2.5. Apoptosis determination

2.5.1. Propidium iodide (PI) and di-amidino phenylindole (DAPI) staining

The compound was more active and selective towards MCF-7 cells, thus, these cells were selected for further studies. The cells treated with compound were subjected to microscopic analysis for apoptosis using previously reported protocols (Rashid et al., 2021). The confluent MCF-7 cells (2×10^5 cells in each well) were incubated with the compound (125 and 250 μg/mL), doxorubicin (5 and 10 μg/mL), and the vehicle, followed by the incubation at 37 °C (5 % CO_2 and 95 % O_2) for 48 h. Following this, the medium was aspirated and breast cancer cells were cleaned with phosphate buffer saline (PBS). After washing, cells were treated with formalin (4 %) and fixed with Triton X–100 (0.1 %) on clean glass slides. After 5 min of incubation at room temperature, 10 μL of PI and DAPI dyes (in equal concentrations of 0.01 mg/mL in PBS) were mixed with the cells and glass slides were further incubated for 10 min in the dark. The images of slides were captured (at 20X magnification) at 493/632 and 350/460 nm for PI and DAPI, respectively using fluorescent microscope (Nikon, Japan).

2.5.2. Intracellular reactive oxygen species (ROS) release

The intracellular ROS release in MCF-7 cells by oleanolic acid (125 and 250 μg/mL), doxorubicin (5 and 10 μg/mL), and the vehicle were assessed, as per the previously described method (Rastogi et al., 2010). Briefly, the MCF-7 cells at the density of 2×10^5 were seeded and grown on microscopic cover slips using 24-well plate. The cells were incubated with the tested samples for 48 h. Further, the cells were cleaned with PBS and fixed. The fixed cells were then treated with 10 μL of dichlorofluorescin diacetate dye. The treated cells were incubated in the dark for 5–10 min at room temperature. The images of cells were captured at 488/530 excitation/emission filters at 20X magnification using fluorescent microscope (Nikon, Japan).

2.5.3. Determination of mitochondrial membrane potential (MMP)

The compromised MMP ($\Delta\Psi m$) was evaluated using JC-1 staining. The MCF-7 cancer cells (2×10^5 cells/well) were plated in 24-well plate with 1 mL of complete media and incubated at 37 °C for 12 h. Further, the confluent MCF7 cells were exposed to 125 μg/mL of oleanolic acid and 10 μg/mL of doxorubicin. After 48 h, medium from each well was aspirated and cells were cleaned with PBS. These cells were then fixed with formalin, and incubated with 10 μL of JC-1 probe for 30 min in a dark at 37 °C. The cells were observed using a fluorescent microscope (Nikon, Japan) at 550/570 nm excitation and emission wavelength (Khan et al., 2021).

2.5.4. Activation of caspase-9 and caspase-7

Caspase-9 and caspase-7 activation potentials of oleanolic acid were assessed using fluorometric assay (Jiao et al., 2020). Briefly, MCF-7 cells (1×10^6 cells/well/3 mL) were scattered in a 6-well plate and incubated at 37 °C in a humid CO_2 environment (5 %). After the overnight incubation, the old cell culture medium was replaced with the fresh medium. Then, the MCF-7 cells were incubated with oleanolic acid (125 and 250 μg/mL). After 12 h of incubation, cells were collected and then centrifuged at 2500 *g* for 10 min at 4 °C. The cells were again suspended in 50 μL of chilled lysis buffer for 15 min. After centrifugation at 10,000 *g*, the cell lysate was collected and protein content was quantified using the Bradford reagent method (Rashid et al., 2021). After protein quantification, the lysate was individually incubated with the substrate for caspase-9 and caspase-7 (Jiao et al., 2020). Afterwards, the reaction buffer was added into the aforementioned lysate mixture and placed at 37 °C for 2 h. An equal volume of reaction buffer, lysis buffer, and substrate was used for the background fluorescence. The amount of fluorescent products were estimated at an excitation/emission wavelength of 400/505 nm using fluorescent microplate reader (FLUOstar Omega, Germany).

2.5.5. Molecular analysis of selected compounds

For molecular analysis, the MCF-7 cancer cell lines were exposed to the vehicle control and isolated compound for 48 h. Total RNA from compound and vehicle-treated cells was extracted using Trizol reagent (TRIzol® reagent, Thermo Fisher Scientific). The extracted RNA was quantified with UV–Visible spectrophotometer (T80 + PG Instruments, Lutterworth, United Kingdom) at 280/260 nm. The cDNA was synthesized using cDNA synthesizing kit by following the manufacturer instructions (WizScript™ cDNA Synthesis Kit, 50 rxn).

Semi-quantitative reverse transcriptase polymerase chain reaction was carried out to evaluate the effects of treatments on *Bcl-2* and *PDGF* expression. For this purpose, the reaction mixture (14.3 μL) was prepared by using 0.7 μL primers (forward and reverse each), 1 μL cDNA, 3.4 μL master mix (PCR buffer 1.5 μL, dNTPs 0.3 μL, $MgCl_2$ 1.2 μL, and Taq 0.4 μL), and 9.2 μL PCR-water (Thermo Scientific). The PCR program was set as 7 min denaturation (hot start at 94 °C), followed by 35 cycles of 30 *sec* denaturation at 94 °C, annealing at 59 °C and 72 °C for 30 *sec*, and final extension for 7 min at 72 °C. PCR amplification was accomplished with *Bcl-2* and *PDGF* primers, as described in the Table 1. Amplicons were separated by the gel electrophoresis (2 % agarose gel), and visualized through ethidium bromide stain using UV-transilluminator (MLB-21. UltraBright). A 100 bp DNA ladder molecular weight marker (GeneOn GmbH, Deutschland, Germany) was run on agarose gel to confirm an expected molecular weight of an amplification product. Finally, the gel images were analyzed through the ImageJ software.

2.6. Statistical analyses

Experiments were performed in triplicate and results were presented as mean ± SD with the confidence interval of 95 %. The *P* value ≤ 0.05 was considered as statistically significant.

Table 1
Sequence of primers and conditions used for semi-quantitative RT-PCR.

Genes	Primers	Sequence	Amplicon size	Annealing temperature
Bcl2	Forward Reverse	ATCGCCCTGTGGATGACTGAG CAGCCAGGAGAAATCAAACAGAGG	129 bp	59 °C
PDGF	Forward Reverse	ACCCAGGAGCTAGGGAAGAG GGGACACAGGCACTTGCTAT	263 bp	59 °C

3. Results

3.1. Isolation and characterization of isolated compound

The repeated silica gel column chromatographic separation of ethyl acetate fraction of *L. stoechas* using *n*-hexane/ethyl acetate as eluent showed white crystalline compound (22 mg). The HPLC chromatogram of the isolated compound showed a peak at the retention time of 8.64 min by applying formic acid in water (0.1 %) (solvent A) and in acetonitrile (solvent B). The mass spectra of the compound displayed the molecular ion peak at *m*/*z* 457.37 $[M + H]^+$, corresponding to a molecular formula of $C_{30}H_{49}O_3$. The MS2 spectrum gave a base peak at 439.4081 with the loss of water molecule [Supplementary Fig. 1 (Fig. S1)]. The fragmentation pattern revealed similarity with triterpenoids. In FT-IR spectrum, the isolated compound showed the characteristic absorption band for —OH (2926.01 cm^{-1}), C=C (1687.71 cm^{-1}), and $-CH_3$ (1454.33 cm^{-1}) (Fig. S2). The ^1H NMR spectra showed the presence of 7 methyl groups at δ 0.68 (3H, H-26), 0.72 (3H, H-24), 0.86 (3H, H-29), 0.88 (3H, H-25), 0.90 (3H, H-30), 1.14 (3H, H-23), and 1.24 (3H, H-27). The spectrum also showed presence of oxygenated methine proton at δ 3.32 (1H, H-3), while the olefinic proton of C12-C13 (distinct characteristic triplet) showed it at δ 5.17 (1H, H-12) (Fig. S3). HSQC spectrum showed a correlation of C-12 (122) with proton H-12 (5.16 ppm). ^1H NMR signals for H-3 (2.99 ppm) correlated to C-3 signals at 77.36 ppm. In HSQC, H-18 (2.76 ppm) showed a correlation to C-18 at 41.39 ppm. The C-27 (26.12 ppm) showed connectivity to H-27 at 1.10 ppm. Proton signals for H-23 (0.98 ppm) correlated to C-23 signals at 27.77 ppm. In HSQC, H-29 (0.88 ppm) showed a correlation to C-29 at 33.32 ppm. HSQC spectrum also showed a correlation of C-26 (16.50) with proton H-26 (0.68 ppm) (Fig. S4). Based on HRMS, MS2, FT-IR, ^1H NMR and 2D NMR data, the isolated compound was characterized as oleanolic acid (Fig. 1).

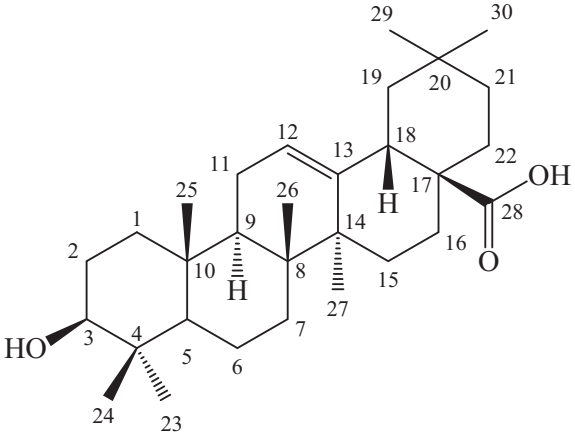

Fig. 1. Structure of oleanolic acid.

3.2. Anti-proliferative activity of oleanolic acid

The anti-proliferative effect of oleanolic acid was assessed on MCF-7, MDA-MB-231, and BHK-21 cell lines. The oleanolic acid exhibited a concentration-dependent anticancer potential with maximum inhibition of 72.44 ± 3.33 and 78.55 ± 2.67 % against MCF-7 (IC_{50} value – 13.09 µg/mL) and MDA-MB-231 (IC_{50} value – 160.22 µg/mL) cell lines, respectively. The oleanolic acid exhibited negligible toxicity towards BHK-21 cells at varied concentrations (Fig. 2). On the other hand, oleanolic acid showed toxicity against MCF-7 and MDA-MB-231 cells with SI values of 38.20 and 3.12, respectively. This data showed that oleanolic acid has more selectivity towards MCF-7 breast carcinoma cells than MDA-MB-231, therefore, these cells were selected for further cytotoxic and apoptotic studies.

3.3. PI and DAPI staining

The PI and DAPI staining of oleanolic acid and doxorubicin treated MCF-7 cells showed cell shrinkage, nuclear condensation, and DNA fragmentation. In contrast, the untreated and vehicle-treated cancer cells showed no changes in its morphology (Fig. 3 and Fig. 4).

3.4. Intracellular ROS production

The capability of oleanolic acid to induce ROS in MCF-7 cancer cells was observed using dichlorofluorescein diacetate that formed a fluorescent product dichlorofluorescein (DCF) in an interaction with ROS. The fluorescence produced in MCF-7 cells was observed by fluorescence microscope under the green filter. The oleanolic acid induced a concentration-dependent ROS production in MCF-7 cancer cells to exhibit its anticancer activity (Fig. 5).

3.5. Loss of MMP

Oleanolic acid and doxorubicin-treated MCF-7 cells showed reduction in red/green ratio (compromised MMP), thereby indicated that the compound targeted mitochondrial contents to accomplish apoptosis in breast cancer cells. The untreated (control) cells showed increased red/green ratio indicating that the control cells maintained normal MMP (Fig. 6).

3.6. Caspase-9 and caspase-7 activation

Results showed that there were about 1.77- and 2.19-fold increments in caspase-9 production (Fig. 7A) and 2.27 and 2.82 folds increments in the production of caspase-7 (Fig. 7B) at 125 and 250 µg/mL, respectively in MCF-7 cells. Similarly, in doxorubicin treated MCF-7 cells, there was about 4.11- and 6.20-fold rise in caspase-9 (Fig. 8A), and 3.34- and 5.47-fold increment in the production of caspase-7 (Fig. 8B) at 5 and 10 µg/mL, respectively.

3.7. Down-regulation of Bcl2 and PDGF expression in compound treated MCF-7 cells

In the current study, *Bcl2* and *PDGF* expression in compound treated breast carcinoma (MCF-7) cells was assessed using poly-

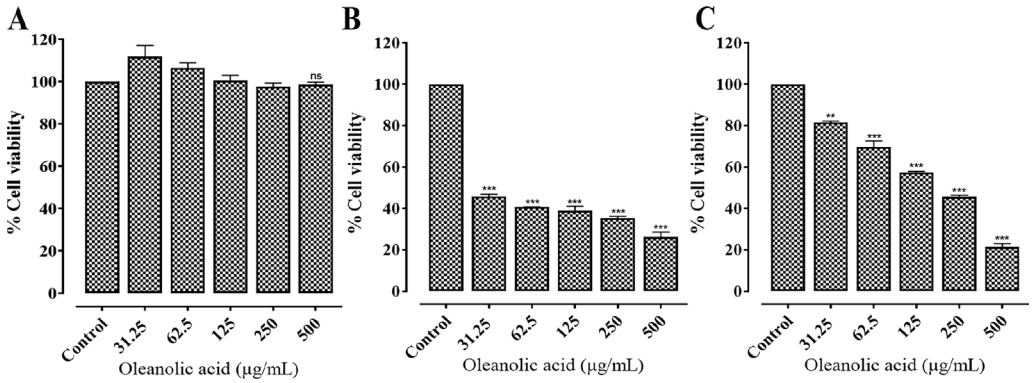

Fig. 2. *In vitro* anti-proliferative activity of oleanolic acid at varied concentrations against (**A**) BHK-21, (**B**) MCF-7, and (**C**) MDA-MB-231 cells. Values represent mean ± SD. ** and *** represent *P* value ≤ 0.01 and ≤ 0.001, respectively.

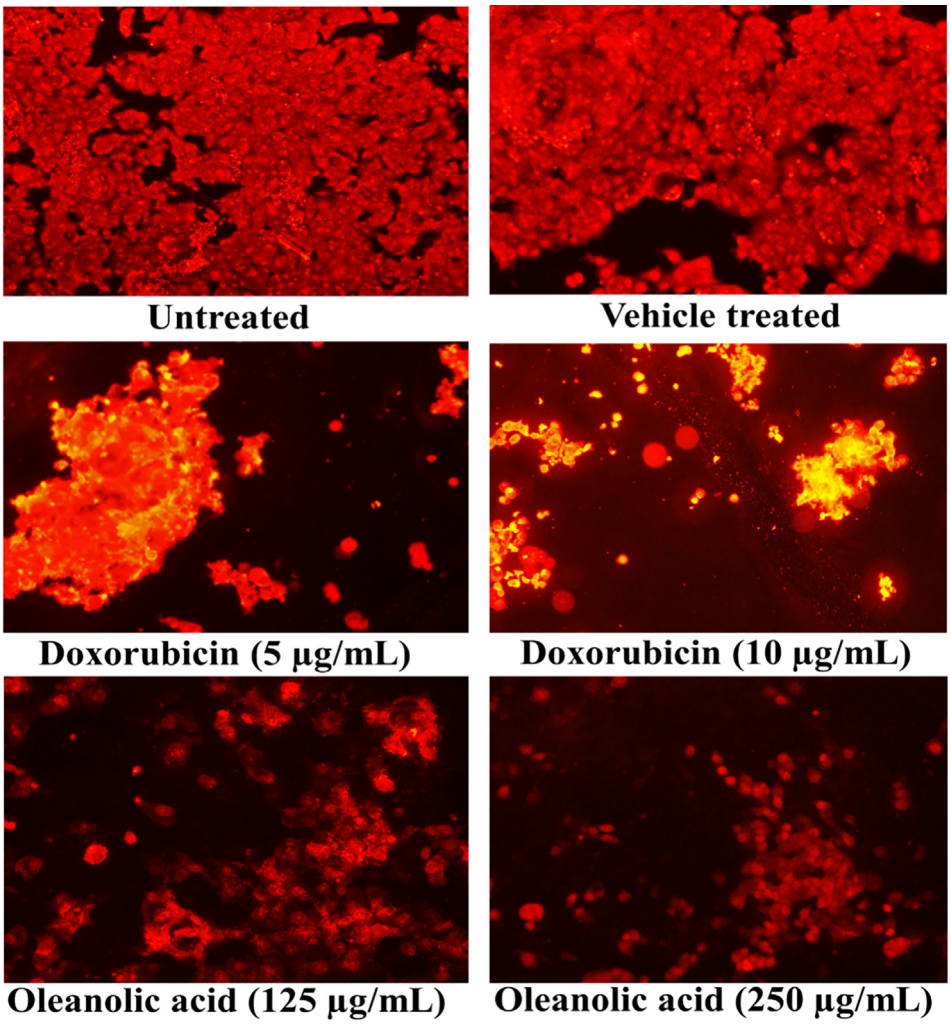

Fig. 3. Cellular morphology of oleanolic acid and doxorubicin-treated MCF-7 cancer cells following PI staining using a fluorescence microscope at 20X.

merase chain reaction (PCR). The PCR results revealed that *Bcl2* and PDGF expression was down-regulated in treated MCF-7 cells. The compound showed 4.43-fold down-regulation of *Bcl2* gene in MCF-7 cells (Fig. 9A). Similarly, the compound also down-regulated the expression of *PDGF* gene (1.40-fold in comparison to control), as shown in Fig. 9B.

4. Discussion

Bioactive natural products may be considered as a very promising starting point for the development of new and novel therapeutic agents (Prasathkumar et al., 2021; Eftekhari et al., 2021; Khuda et al., 2022; Faheem et al., 2022). Drugs like anti-malarial quinine

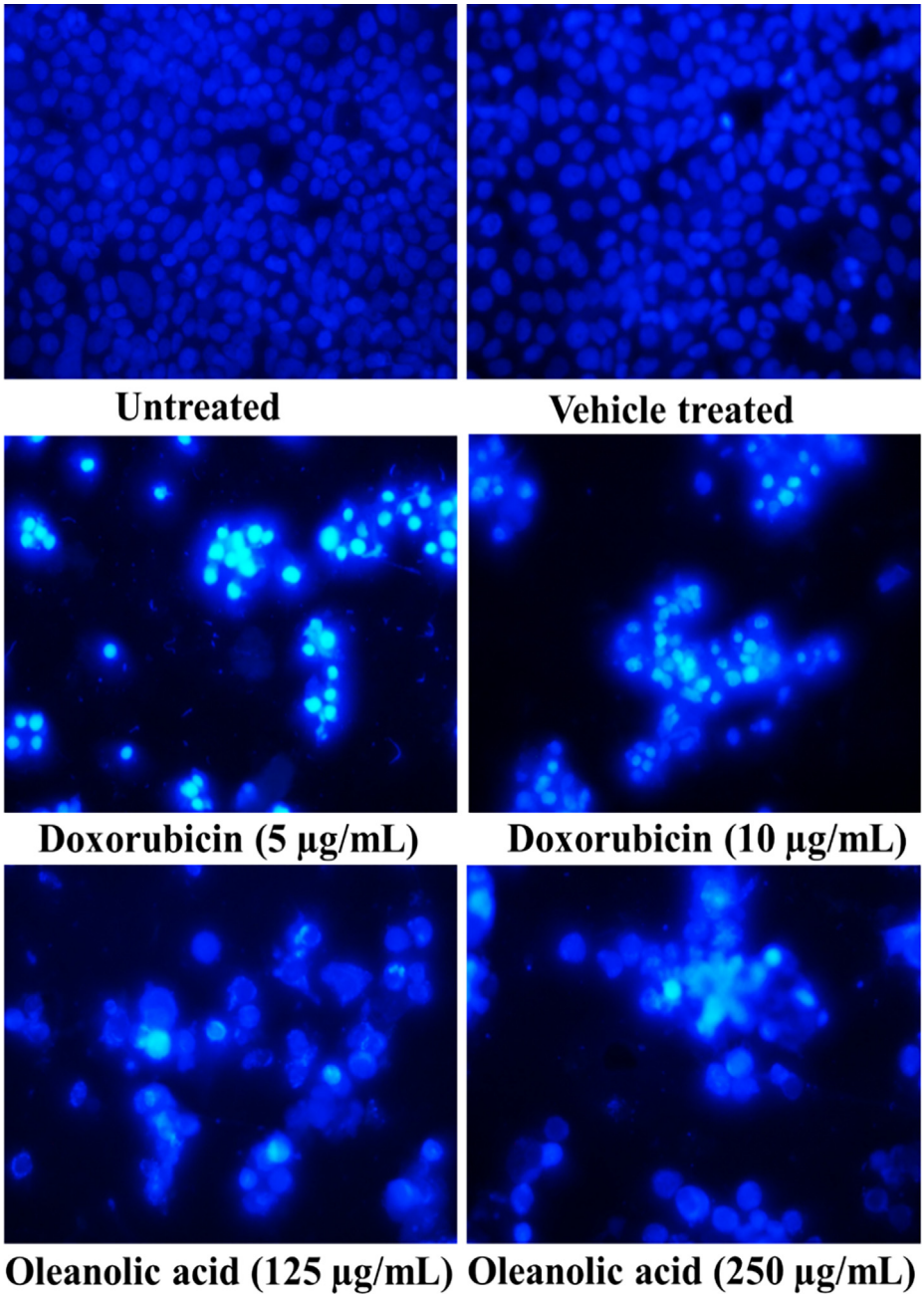

Fig. 4. Cellular morphology of oleanolic acid and doxorubicin-treated MCF-7 cancer cells following DAPI staining using a fluorescence microscope at 20X.

and artemisinin, digoxin (widely used in cardiovascular diseases), the anticancer drug paclitaxel, and the analgesics morphine, codeine, and acetyl salicylic acid have all been derived from natural products, which validates that the natural products have a leading role in lead discovery for the development of remedies against human diseases (Newman and Cragg, 2007). One of the major classes of natural compounds better known for medicinal values is terpenoids. These are the most widespread and the largest class of secondary metabolites present mainly in plants, algae, mosses, lichens, liverworts, and marine organisms or other microbes. A few of these terpenoids have been utilized for therapeutic applications for centuries as antibacterial, anti-inflammatory, and antitumoral agents (Chakraborty et al., 2022). However, in recent times, level of research activity on these compounds has constantly increased. In this study, a natural terpenoid (oleanolic acid) was isolated from the ethyl acetate fraction of *L. stoechas* (based on LC-MS/MS profile of extract and ethyl acetate fraction). The structure elucidation of isolated compound was carried out through modern spectroscopic techniques including HRMS, MS2, FT-IR, ^{1}H NMR, and 2D NMR and the compound was further proceed for detailed mechanistic study for anticancer activity.

In the present study, oleanolic acid exhibited not only a concentration-dependent cytotoxic activity against MCF-7 and MDA-MB-231 cancer cells, but also showed negligible toxicity towards non-cancer cells. The selectivity of the compounds may be ascertained by their SI. The SI > 3 of the compound indicates that it has selective toxicity to cancer cells, while SI < 3 for compounds is considered toxic to non-cancerous cells (Awang et al., 2014). In this study, oleanolic acid showed toxicity against MCF-7 and MDA-MB-231 cell lines with high SI values. These results proposed that oleanolic acid is non-toxic to normal cells and may be utilized as a potent anticancer agent against breast cancer.

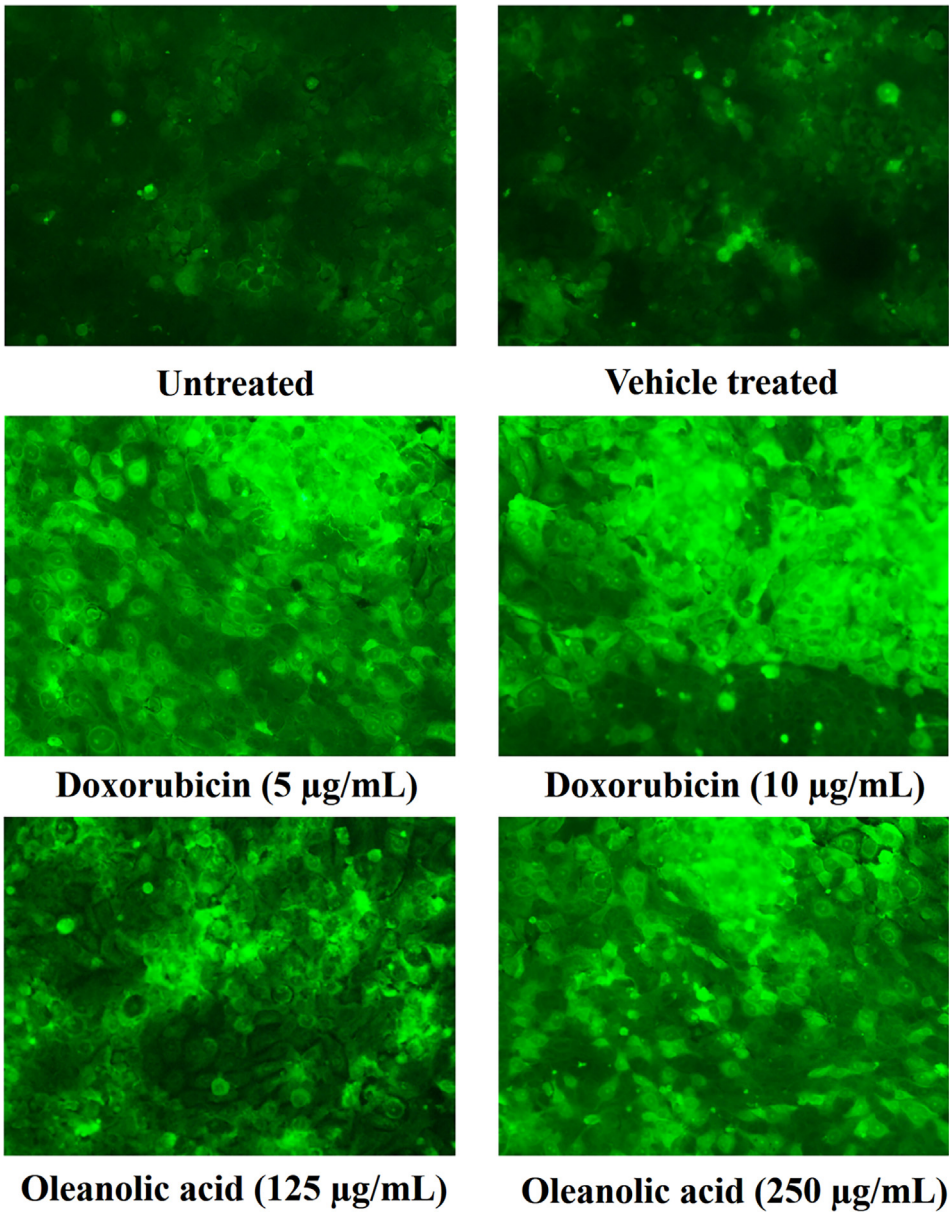

Fig. 5. Fluorescence formed by an oxidized DCF as an outcome of ROS production by oleanolic acid in MCF-7 cancer cells using a fluorescence microscope at 20X.

MCF-7 and MDA-MB-231 cell lines have been widely studied for anti-breast cancer activity of extracts or compounds. In this present study, oleanolic acid showed more selectivity towards MCF-7 cells than MDA-MB-231 (triple-negative breast cancer cells). Therefore, MCF-7 cells were selected for further cytotoxic, pro-apoptotic, ROS generation, MMP, caspase activation, and molecular studies.

PI is the fluorescence producing agent that attaches with the DNA of non-living cells, as plasma membrane of these deceased cells becomes permissible pathway for foreign particles. Likewise, the DAPI staining is employed to determine apoptosis in cancer cells (Rashid et al., 2021). In this context, the morphological observations through PI staining showed a dose-dependent reduction in the cell population and appearance of yellowish red fluorescence in apoptotic breast cancer cells, which confirmed the cytotoxic effect of oleanolic acid. Apoptotic cells have characteristic features like nuclear fragmentation, chromatin condensation, membrane blebbing, and establishment of apoptotic bodies (Doonan and Cotter, 2008). In DAPI staining, an increase in bluish fluorescence indicated the binding of the dye with DNA after penetration into the cells due to the increased membrane permeability. Additionally, nuclear condensation and cell shrinkage were observed in treated cancer cells in comparison to the control cells, which confirmed the pro-apoptotic potential of oleanolic acid.

ROS is generally produced in mitochondria in small amount and plays a vital role in various signaling pathways. The higher ROS levels are lethal to the cells (Perillo et al., 2020). Therefore, cancer cells are more prone to apoptosis in comparison to the normal cells when treated with ROS-inducing agents (Reczek and Chandel, 2017). In the present study, oleanolic acid (125 and 250 µg/mL) was used for evaluating its effect on oxidative stress. The oleanolic acid represented a dose dependent increment in ROS level at higher dose. Oleanolic acid has been reported to cause up-regulation of Bax protein in treated cancer cells (Kim et al., 2018). Bax is associated with poration of the mitochondrial membrane (Westphal et al., 2014) and over production of ROS in cancer cells. Excessive mitochondrial activity in cancer cells leads to an increased ROS generation (Perillo et al., 2020). The ROS generation

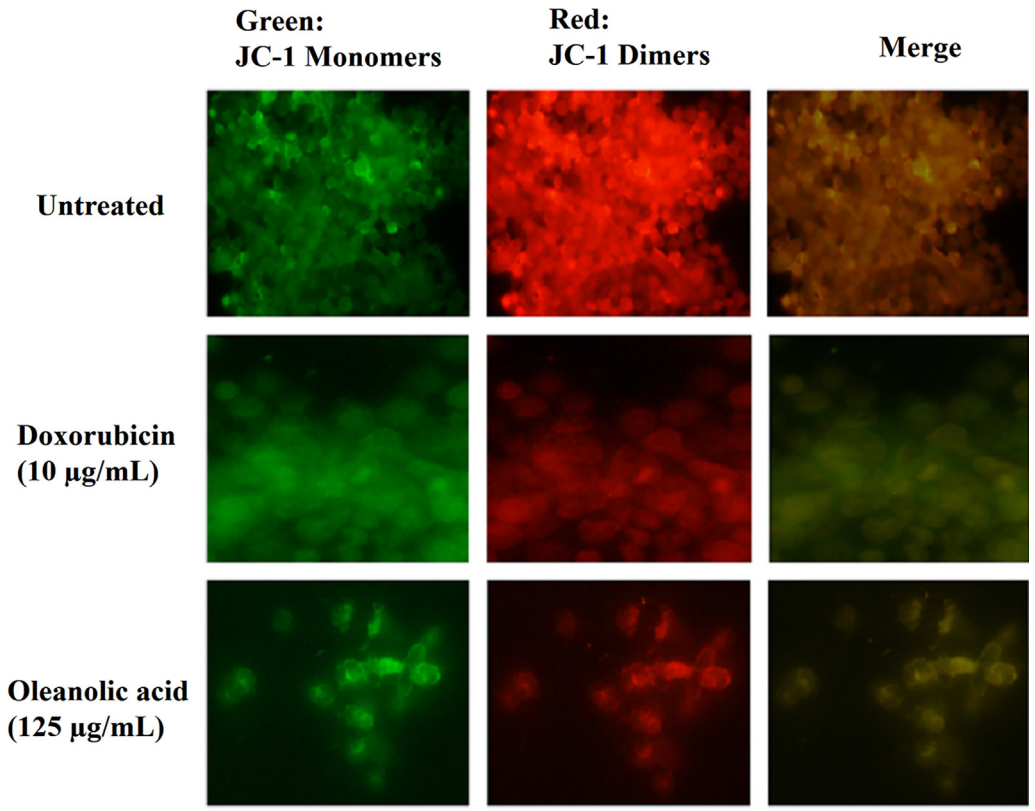

Fig. 6. Depolarization of MMP in oleanolic acid-, doxorubicin-treated, and untreated (control) MCF-7 cancer cells by detecting the ratio of red to green fluorescence followed by JC-1 stain.

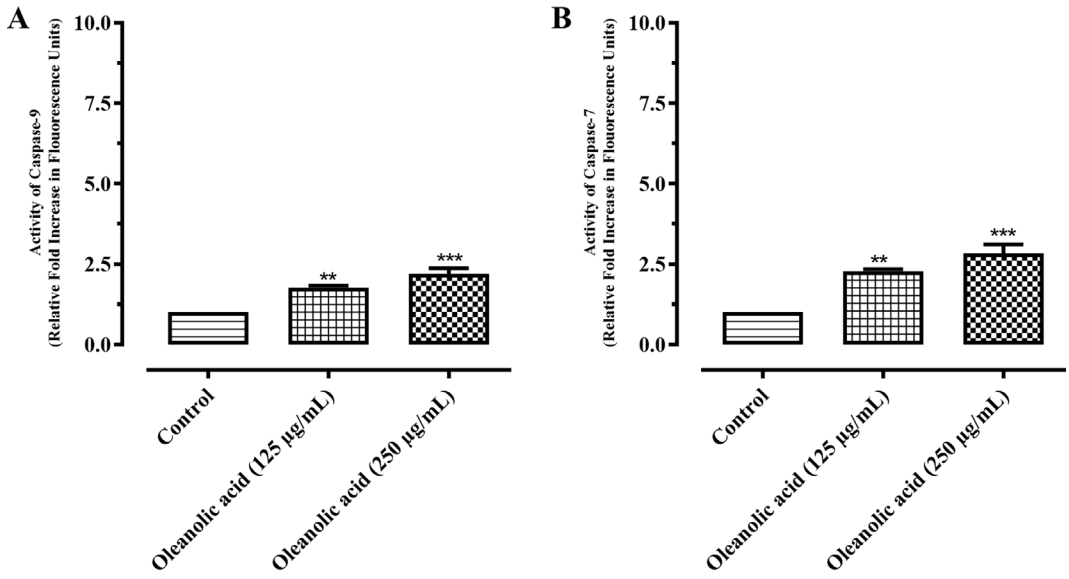

Fig. 7. Activation of (**A**) caspase-9 and (**B**) caspase-7 in MCF-7 cancer cells after treatment with oleanolic acid. Values are expressed as mean ± SD. ** and *** represent *P* value $\leq$ 0.01 and $\leq$ 0.001, respectively.

in this study is similar to the other study as reported previously for another compound (Chen et al., 2010). In another study, oleanolic acid has induced oxidative stress in HepG2 cells (Wang et al., 2013), whereas other studies revealed reduced or negligible ROS generation in breast cancer cells (Sánchez-Quesada et al., 2015). In the current study, higher concentration and long incubation time of cells were employed that might be the possible reason for the ROS generation potential of oleanolic acid in MCF-7 cells. In short, oleanolic acid has ROS inducing activity as well as ROS scavenging activity that might be dependent on source, cell type, and dose of oleanolic acid used.

The mitochondrial dysfunction in the cancer cells is attaining popularity among researchers, and thus, molecules aiming mitochondrial pathway are being discovered (Lu et al., 2016). JC-1 (fluorescent probe) is commonly used for the detection of MMP in cells or tissues (Tai et al., 2016). JC-1 is a green fluorescent stain and

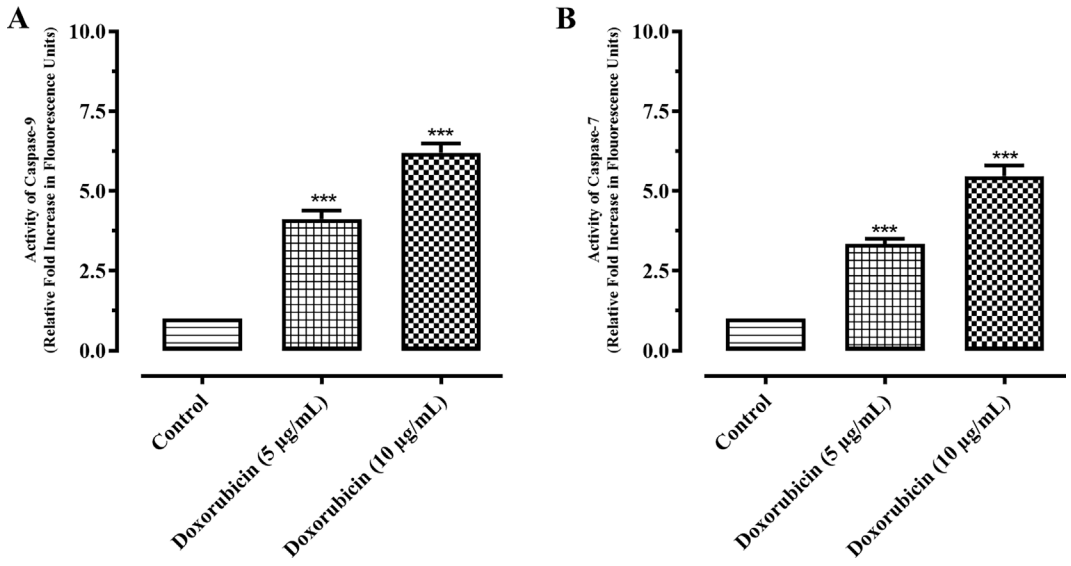

Fig. 8. Activation of (**A**) caspase-9 and (**B**) caspase-7 in MCF-7 cancer cells after treatment with doxorubicin. Results are expressed as mean ± SD. *** represent *P* value ≤ 0.001.

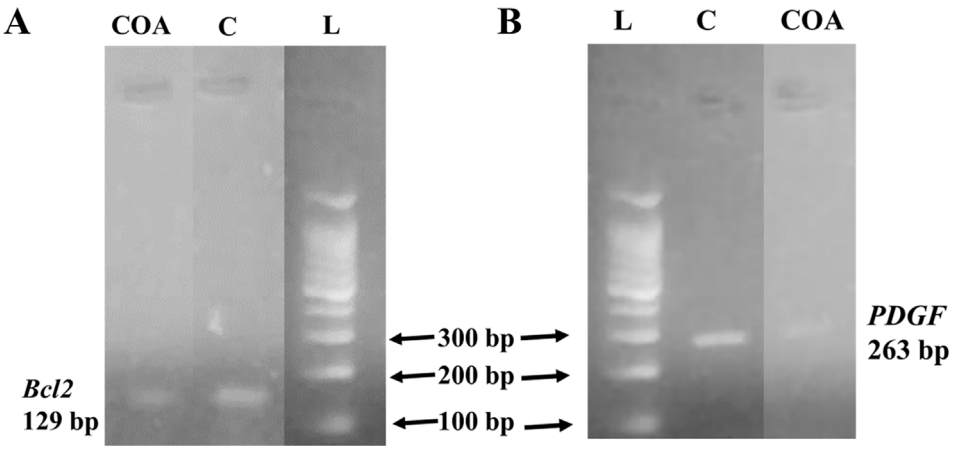

Fig. 9. Comparison of *Bcl2* mRNA expression (**A**) and *PDGF* mRNA expression (**B**) level in compound-treated MCF-7 cells. L, C, and COA represent ladder, control, and oleanolic acid lanes, respectively.

when the MMP is increased (in live cells), JC-1 accumulates in mitochondria. In this study, it was converted to J-aggregates by the mitochondrial enzymes and produced red fluorescence. Contrarily, when MMP is reduced in dead cells, JC-1 can not be converted to J-aggregates. Therefore, there is no change in the color, and thus, green fluorescence is produced (Baxa et al., 2005). Therefore, MMP can be easily determined based on fluorescence color change. A significant reduction in MMP is an ideal sign of an early apoptosis. The current study revealed an intense green fluorescence in oleanolic acid-treated MCF-7 cancer cells as compared to red fluorescence in untreated cells, which is an indicative of early apoptosis due to mitochondrial dysfunction. The results of the current study are in accordance with a previous report (Pandey et al., 2019).

Caspases (cysteine proteases) are the enzymes, which are mostly activated in an apoptotic cascade. Later, the discharge of cytochrome-c from mitochondrial outer membrane leads to the stimulation of initiator (caspase-8 and caspase-9) and executioner (caspase-3 and caspase-7) caspases, and therefore, persuades apoptosis (Degterev et al., 2003). In the current investigation, caspase activation assay was performed to confirm the intrinsic pathway of apoptosis. The findings revealed about 2-fold increments in caspase-9 production and 3-fold increase in the production of caspase-7 in MCF-7 cancer cells. Findings revealed potential role of oleanolic acid in the induction of apoptosis via mitochondrial pathway (intrinsic arm of apoptosis).

Bcl-2 is a part of protein families that have a very crucial role in the regulation of cell apoptosis. *Bcl-2* is the proto-oncogene which is when over-expressed leads to the inhibition of cell apoptosis (Beck et al., 2002). It suppresses the cell death by inhibiting release of cytochrome-c, which is the major component of the cell respiration from the mitochondria. Eventually, it inhibits the activation of caspases that are actor proteins and plays a vital role in the initiation and sustaining of apoptosis (Kumar et al., 2000; El-Maksoud et al., 2021). In breast cancer cell, *Bax* (inhibitor of the *Bcl-2*) and *Bcl-2* are constitutively expressed to tightly regulate the apoptosis (Kumar et al., 2000; Beck et al., 2002). One of the many factors in breast carcinomas is up-regulation of *Bcl-2* gene, which ultimately results in the inhibition of apoptosis (Beck et al., 2002). It has been well reported that the inhibition of *Bcl-2* and *Bcl-xL* expression and their anti-apoptotic functions may help to increase the efficacy of chemotherapeutic agents (Kumar et al., 2000). The current study

revealed that oleanolic acid remarkably decreased the *Bcl-2* expression in MCF-7 cell line. It is therefore, clear that this compound induced apoptosis in MCF-7 cells, via intrinsic pathways.

Platelet-derived growth factor (*PDGF*) receptor signaling pathway is over-activated or altered in various cancers like prostate, pancreatic, and lung cancers (Pinto et al., 2014). However, breast adenocarcinoma patients have increased level of vascular endothelial growth factor and *PDGF* in tumors and serum as compared to the controls (Rykala et al., 2011). Therefore, it is possible that anti-*PDGF* receptor remedies will be required for such patients. These therapies should be selected on the basis of clearly defined criteria for the presence of *PDGF* receptors on their cancer cells (Pinto et al., 2014). In this study, oleanolic acid considerably down-regulated the expression of *PDGF* gene in MCF-7 breast cancer cells. To the best of our knowledge and reported literature, this study is a first report on the anti-*PDGF* mechanism of oleanolic acid in MCF-7 cells. Therefore, these data suggest that oleanolic acid might be used as lead compound for the development of anti-*PDGF* breast cancer drugs.

5. Conclusions

The isolated compound, oleanolic acid was characterized and confirmed by FT-IR, ESI-HRMS, and NMR. Oleanolic acid showed anticancer properties against MCF-7 and MDA-MB-231 cell lines. The compound favored apoptotic mechanism in MCF-7 cell that was observed through fluorescent microscopy (PI and DAPI staining), increased ROS generation, compromised mitochondrial function, involvement of caspase-9 and caspase-7 stimulation, and down-regulation of *Bcl2* and *PDGF* genes. Findings revealed the promising anticancer properties of oleanolic acid against MCF-7 cells by induced apoptosis process. This study depicted that oleanolic acid was more selective towards breast cancer cells than the standard drug, and it might serve as a lead compound for developing relatively safer chemotherapeutic agents in breast cancer management. Moreover, oleanolic acid may be explored for other targets (aromatase inhibition and breast cancer genes) in breast cancer cells for the development of anticancer drugs. The least cytotoxic effect of oleanolic acid was non-cancerous BHK-21 cells has revealed the ever needed safety of an anticancer agent. In addition, this safety gain can draw the attention of many herbal and nutraceutical industries in developing the anti-breast cancer formulations.

Declaration of Competing Interest

The authors declare that they have no known competing financial interests or personal relationships that could have appeared to influence the work reported in this paper.

Acknowledgements

The authors are thankful to Prof. Dr. Jamshed Iqbal, Centre for Advanced Drug Research, COMSATS University Islamabad, Abbottabad Campus for providing the facilities for fluorescent microscopy. The authors like to thank Taif University, Taif, Saudi Arabia, for their support (Taif University Researchers Supporting Project number: TURSP-2020/80). M.G. was supported by the János Bolyai Research Scholarship (BO/00144/20/5) of the Hungarian Academy of Sciences. The research was supported by the ÚNKP-21-5-540-SZTE New National Excellence Program of the Ministry for Innovation and Technology from the source of the National Research, Development and Innovation Fund.

Appendix A. Supplementary material

Supplementary data to this article can be found online at https://doi.org/10.1016/j.jksus.2022.102454.

References

Awang, N., Aziz, Z.A., Kamaludin, N.F., Chan, K.M., 2014. Cytotoxicity and mode of cell death induced by Triphenyltin (IV) compounds *in vitro*. J. Biol. Sci. 14, 84–93.

Batool, A., Miana, G.A., Alam, M., Khan, M.T., Muddassir, M., Zaman, W., et al., 2022. Bioassay-guided fractionation and isolation of Arctigenin from *Saussurea heteromalla* for *in vitro* and *in silico* cytotoxic activity against HeLa cells. Physiol. Mol. Plant Pathol. 117,. https://doi.org/10.1016/j.pmpp.2021.101749 101749.

Baxa, D.M., Luo, X., Yoshimura, F.K., 2005. Genistein induces apoptosis in T lymphoma cells via mitochondrial damage. Nutr. Cancer. 51, 93–101.

Beck, M.T., Peirce, S.K., Chen, W.Y., 2002. Regulation of bcl-2 gene expression in human breast cancer cells by prolactin and its antagonist, hPRL-G129R. Oncogene 21, 5047–5055.

Bines, J., Eniu, A., 2008. Effective but cost-prohibitive drugs in breast cancer treatment. Cancer 113, 2353–2358.

Chakraborty, A.J., Uddin, T.M., Zidan, B.M.R.M., Mitra, S., Das, R., Nainu, F., et al., 2022. Allium cepa: a treasure of bioactive phytochemicals with prospective health benefits. Evid.-based Complement. Altern. Med. https://doi.org/10.1155/2022/4586318.

Chen, Z., Jin, K., Gao, L., Lou, G., Jin, Y., Yu, Y., Lou, Y., 2010. Anti-tumor effects of bakuchiol, an analogue of resveratrol, on human lung adenocarcinoma A549 cell line. Eur. J. Pharmacol. 643, 170–179.

Degterev, A., Boyce, M., Yuan, J., 2003. A decade of caspases. Oncogene 22, 8543–8567.

Doonan, F., Cotter, T.G., 2008. Morphological assessment of apoptosis. Methods 44, 200–204.

Eftekhari, A., Khusro, A., Ahmadian, E., Dizaj, S.M., Dinparast, L., Bahadori, M.B., et al., 2021. Phytochemical and nutra-pharmaceutical attributes of *Mentha* spp.: a comprehensive review. Arab. J. Chem. 14,. https://doi.org/10.1016/j.arabjc.2021.103106 103106.

El-Maksoud, A.A.A., Makhlouf, A.I.A., Altemimi, A.B., El-Ghany, I.H.A., Nassrallah, A., Cacciola, F., Abedelmaksoud, T.G., 2021. Nano milk protein-mucilage complexes: Characterization and anticancer effect. Molecules 26, 6372.

Faheem, M., Ameer, S., Khan, A.W., Haseeb, M., Raza, Q., Shah, F.A., et al., 2022. A comprehensive review on antiepileptic properties of medicinal plants. Arab. J. Chem. 15,. https://doi.org/10.1016/j.arabjc.2021.103478 103478.

Gala, H., Miller, D.A., Williams III, R.O., 2020. Harnessing the therapeutic potential of anticancer drugs through amorphous solid dispersions. Biochim. Biophys. Acta 1873, 188319.

He, L., Wang, X., Ma, Q., Zhao, W., Jia, Y., Dong, G., Zhu, Y., Jia, X., Tong, Z., 2020. Glycyrrhizin inhibits the invasion and metastasis of breast cancer cells via upregulation of expressions of miR-200c and e-cadherin. Trop. J. Pharm. Res. 19, 1807–1813.

Jiao, C., Chen, W., Tan, X., Liang, H., Li, J., Yun, H., He, C., Chen, J., Ma, X., Xie, Y., Yang, B.B., 2020. *Ganoderma lucidum* spore oil induces apoptosis of breast cancer cells *in vitro* and *in vivo* by activating caspase-3 and caspase-9. J. Ethnopharmacol. 247, 112256.

Khan, I., Zaib, S., Javed, M., Rashid, F., Iqbal, J., Ibrar, A., 2021. Antiproliferative and pro-apoptotic effects of thiazolo[3,2-b][1,2,4]triazoles in breast and cervical cancer cells. Anticancer Agents Med. Chem. 21, 2181–2191.

Khuda, F., Anjum, M., Khan, S., Khan, H., Sahibzad, M.U.K., Khusro, A., et al., 2022. Antimicrobial, anti-inflammatory and antioxidant activities of natural organic matter extracted from cretaceous shales in district Nowshera-Pakistan. Arab. J. Chem. 15,. https://doi.org/10.1016/j.arabjc.2021.103633 103633.

Khwaza, V., Oyedeji, O.O., Aderibigbe, B.A., 2020. Ursolic acid-based derivatives as potential anti-cancer agents: an update. Int. J. Mol. Sci. 21, 5920.

Kim, G.J., Jo, H.J., Lee, K.J., Choi, J.W., An, J.H., 2018. Oleanolic acid induces p53-dependent apoptosis via the ERK/JNK/AKT pathway in cancer cell lines in prostatic cancer xenografts in mice. Oncotarget 9, 26370–26386.

Kumar, R., Vadlamudi, R.K., Adam, L., 2007. Apoptosis in mammary gland and cancer. Endocr.- Relat Cancer 7, 257–269.

Latha, R., Rajanathan, T.M.C., Khusro, A., Chidambaranathan, N., Agastian, P., Nagarajan, S., 2019. Anticancer activity of *Mahonia leschenaultii* methanolic root extract and berberine on Dalton's ascitic lymphoma in mice. Asian Pac. J. Trop. Med. 12, 264–271.

Li, X., Song, Y., Zhang, P., Zhu, H., Chen, L., Xiao, Y., Xing, Y., 2015. Oleanolic acid inhibits cell survival and proliferation of prostate cancer cells *in vitro* and *in vivo* through the PI3K/Akt pathway. Tumor Biol. 37, 7599–7613.

Lu, P., Bruno, B.J.R., Lim, C.S., 2016. Delivery of drugs and macromolecules to the mitochondria for cancer therapy. J. Control. Release 240, 38–51.

Nana, W.Y., Ateufack, G., Mbiantcha, M., Khan, S., Rasheed, H.M., Atsamo, A., Shah, A. J., Kamanyi, A., Khan, T., 2019. Antidiarrheal potential of *Distemonanthus benthamianus* Baillon. extracts via inhibiting voltage-dependent calcium channels and cholinergic receptors. Asian Pac. J. Trop. Biomed. 9, 449–455.

Newman, D.J., Cragg, G.M., 2007. Natural products as sources of new drugs over the last 25 years. J. Nat. Prod. 70, 461–477.

Pandey, P., Singh, D., Hasanain, M., Ashraf, R., Maheshwari, M., Choyal, K., Singh, A., Datta, D., Kumar, B., Sarkar, J., 2019. 7-Hydroxyfrullanolide, isolated from *Sphaeranthus indicus*, inhibits colorectal cancer cell growth by p53 dependent and independent mechanism. Carcinogenesis 40, 791–804.

Perillo, B., Donato, M.D., Pezone, A., Zazzo, E.D., Giovannelli, P., Galasso, G., Castoria, G., Migliaccio, A., 2020. ROS in cancer therapy: the bright side of the moon. Exp. Mol. Med. 52, 192–203.

Petrovska, B.B., 2012. Historical review of medicinal plants' usage. Pharmacogn. Rev. 6, 1–5.

Pinto, M.P., Dye, W.W., Jacobsen, B.M., Horwitz, K.B., 2014. Malignant stroma increases luminal breast cancer cell proliferation and angiogenesis through platelet-derived growth factor signaling. BMC Cancer 14, 735.

Prasathkumar, M., Raja, K., Vasanth, K., Khusro, A., Sadhasivam, S., Sahibzada, M.U. K., et al., 2021. Phytochemical screening and *in vitro* antibacterial, antioxidant, anti-inflammatory, anti-diabetic, and wound healing attributes of *Senna auriculata* (L.) Roxb. leaves. Arab. J. Chem. 14,. https://doi.org/10.1016/j.arabjc.2021.103345 103345.

Rasheed, H.M., Wahid, F., Ikram, M., Qaisar, M., Shah, A.J., Khan, T., 2021. Chemical profiling and anti-breast cancer potential of hexane fraction of *Sphaeranthus indicus* flowers. Trop. J. Pharm. Res. 20, 1931–1939.

Rashid, F., Uddin, N., Ali, S., Haider, A., Tirmizi, S.A., Diaconescu, P.L., Iqbal, J., 2021. New triorganotin(IV) compounds with aromatic carboxylate ligands: synthesis and evaluation of the pro-apoptotic mechanism. RSC Adv. 11, 4499–4514.

Rastogi, R.P., Singh, S.P., Häder, D.P., Sinha, R.P., 2010. Detection of reactive oxygen species (ROS) by the oxidant-sensing probe 2′, 7′-dichlorodihydrofluorescein diacetate in the cyanobacterium *Anabaena variabilis* PCC 7937. Biochem. Biophys. Res. Comm. 397, 603–607.

Reczek, C.R., Chandel, N.S., 2017. The two faces of reactive oxygen species in cancer. Annu. Rev. Cancer Biol. 1, 79–98.

Rykala, J., Przybylowska, K., Majsterek, I., Pasz-Walczak, G., Sygut, A., Dziki, A., Kruk-Jeromin, J., 2011. Angiogenesis markers quantification in breast cancer and their correlation with clinicopathological prognostic variables. Pathol. Oncol. Res. 17, 809–817.

Said, A., Naeem, N., Siraj, S., Khan, T., Javed, A., Rasheed, H.M., Sajjad, W., Shah, K., Wahid, F., . Mechanisms underlying the wound healing and tissue regeneration properties of *Chenopodium album*. 3 Biotech 10, 1–10.

Sánchez-Quesada, C., López-Biedma, A., Gaforio, J.J., 2015. Oleanolic acid, a compound present in grapes and olives, protects against genotoxicity in human mammary epithelial cells. Molecules 20, 13670–13688.

Shanmugam, M.K., Dai, X., Kumar, A.P., Tan, B.K.H., Sethi, G., Bishayee, A., 2014. Oleanolic acid and its synthetic derivatives for the prevention and therapy of cancer: preclinical and clinical evidence. Cancer Lett. 346, 206–216.

Siddiqui, M.A., Khalid, M., Akhtar, J., Siddiqui, H., Ahmad, U., Ahsan, F., Khan, M.M., Ahamd, M.Z., Ali, A., 2016. *Lavandula stoechas* (Ustukhuddus): a miracle plant. J. Innov. Pharm. Biol. Sci. 3, 96–102.

Siegel, R.L., Miller, K.D., Jemal, A., 2015. Cancer statistics, 2015. CA Cancer J. Clin. 65, 5–29.

Sporikova, Z., Koudelakova, V., Trojanec, R., Hajduch, M., 2018. Genetic markers in triple-negative breast cancer. Clin. Breast Cancer 18, e841–e850.

Tai, Y., Sun, Y.M., Zou, X., Pan, Q., Lan, Y.D., Huo, Q., Zhu, J.W., Guo, F., Zheng, C.Q., Wu, C.Z., Liu, H., 2016. Effect of *Polygonatum odoratum* extract on human breast cancer MDA-MB-231 cell proliferation and apoptosis. Exp. Ther. Med. 12, 2681–2687.

Wang, X., Bai, H., Zhang, X., Liu, J., Cao, P., Liao, N., Zhang, W., Wang, Z., Hai, C., 2013. Inhibitory effect of oleanolic acid on hepatocellular carcinoma via ERK–p53-mediated cell cycle arrest and mitochondrial-dependent apoptosis. Carcinogenesis 34, 1323–1330.

Westphal, D., Kluck, R.M., Dewson, G., 2014. Building blocks of the apoptotic pore: how Bax and Bak are activated and oligomerize during apoptosis. Cell Death Diff. 21, 196–205.

Zhang, P., Li, H., Chen, D., Ni, J., Kang, Y., Wang, S., 2007. Oleanolic acid induces apoptosis in human leukemia cells through caspase activation and poly(ADP-ribose) polymerase cleavage. Acta Biochim Biophys Sin (Shanghai) 39, 803–809.

Ziberna, L., Šamec, D., Mocan, A., Nabavi, S.F., Bishayee, B., Farooqi, A.A., Sureda, A., Nabavi, S.M., 2017. Oleanolic acid alters multiple cell signaling pathways: implication in cancer prevention and therapy. Int. J. Mol. Sci. 18, 643.